Supplementary Information

An artificial visual neuron with multiplexed rate and time-to-first-spike coding

Fanfan Li[1,2]†, Dingwei Li[2]†, Chuanqing Wang[2]†, Guolei Liu[2], Rui Wang[3], Huihui Ren[2], Yingjie Tang[2], Yan Wang[2], Yitong Chen[2], Kun Liang[2], Qi Huang[4], Mohamad Sawan[2,4,5], Min Qiu[2,4,5], Hong Wang[3]*, Bowen Zhu[2,4,5]*

†These authors contributed equally to this work.

[1]Zhejiang University, Hangzhou 310027, China.

[2]Key Laboratory of 3D Micro/Nano Fabrication and Characterization of Zhejiang Province, School of Engineering, Westlake University, Hangzhou 310024, China.

[3]Key Laboratory of Wide Band Gap Semiconductor Technology, School of Microelectronics, Xidian University, Xi'an, 710071 China.

[4]Westlake Institute for Optoelectronics, Westlake University, Hangzhou 311421, China.

[5]Institute of Advanced Technology, Westlake Institute for Advanced Study, Hangzhou 310024, China

*Corresponding authors. Email: zhubowen@westlake.edu.cn (B.Z.); hongwang@xidian.edu.cn (H.W.)

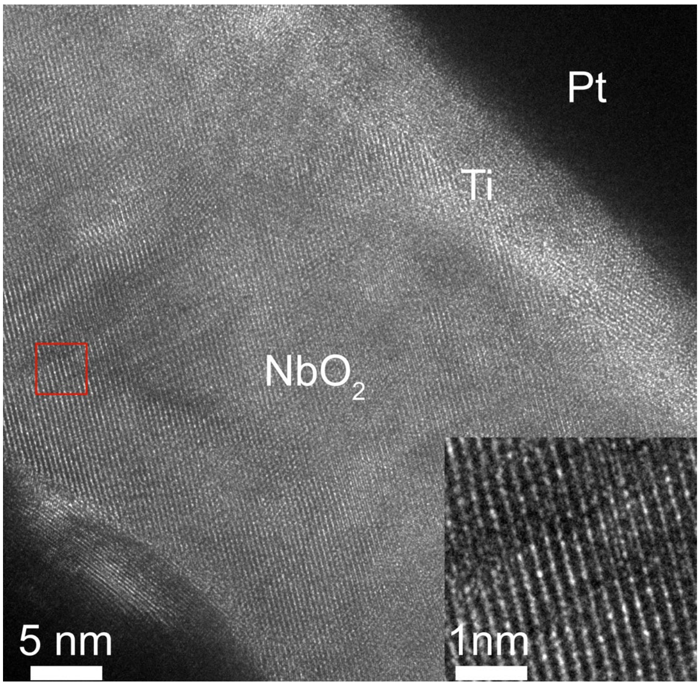

Supplementary Fig. 1. Transmission electron microscopy (TEM) image of the NbO_x Mott memristor. Inset shows high resolution TEM image corresponding to the red square area, showing locally crystallized region of NbO_2.

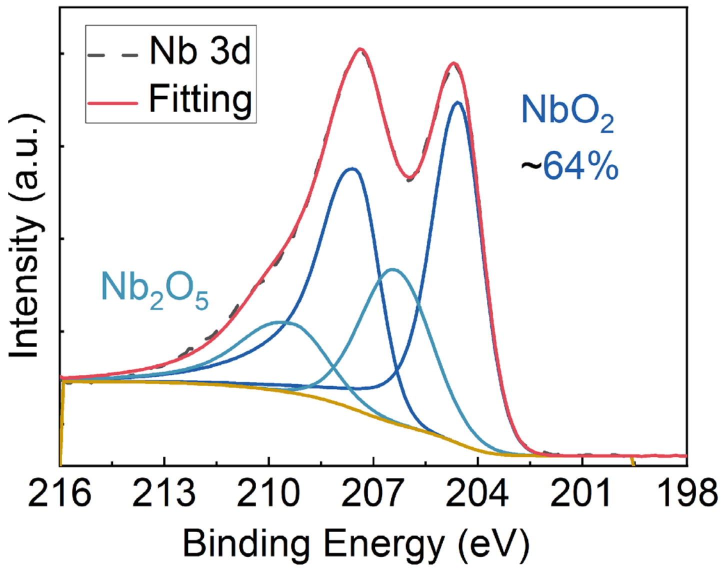

Supplementary Fig. 2. X-ray photoelectron spectroscopy (XPS) analysis of NbO_x films.

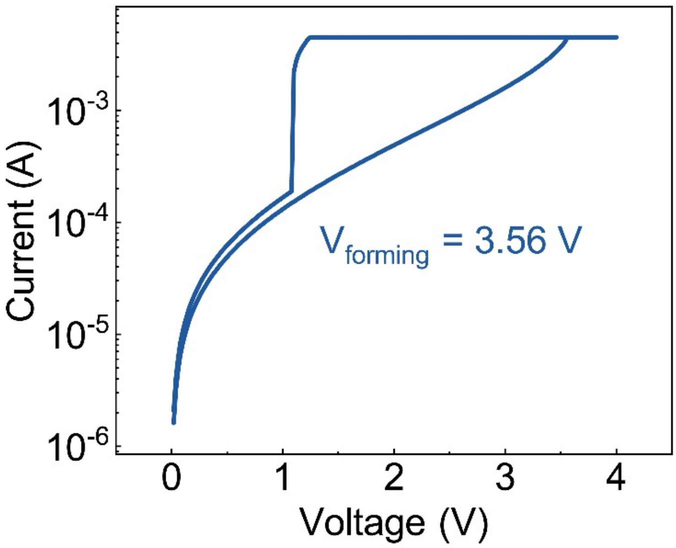

Supplementary Fig. 3. Electroforming operation of the NbO_x memristor. A forming voltage with a compliance current of 4 mA was applied to activate reproducible threshold switching behaviors.

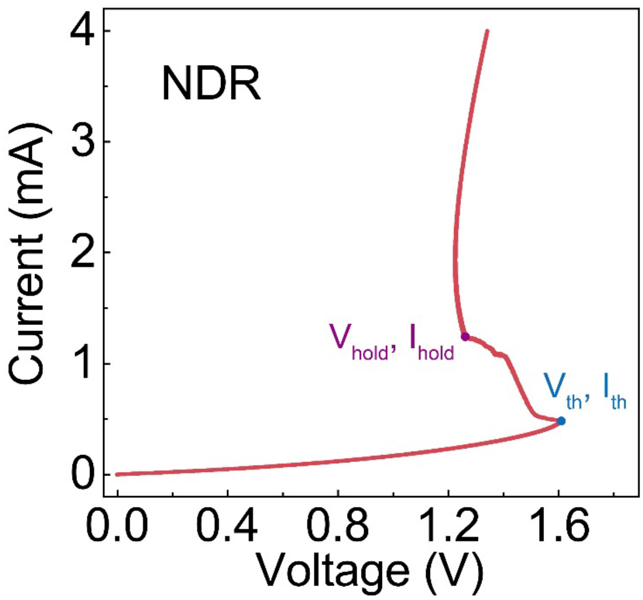

Supplementary Fig. 4. Current-programmed negative differential resistance (NDR) characteristics of the NbO_x memristor.

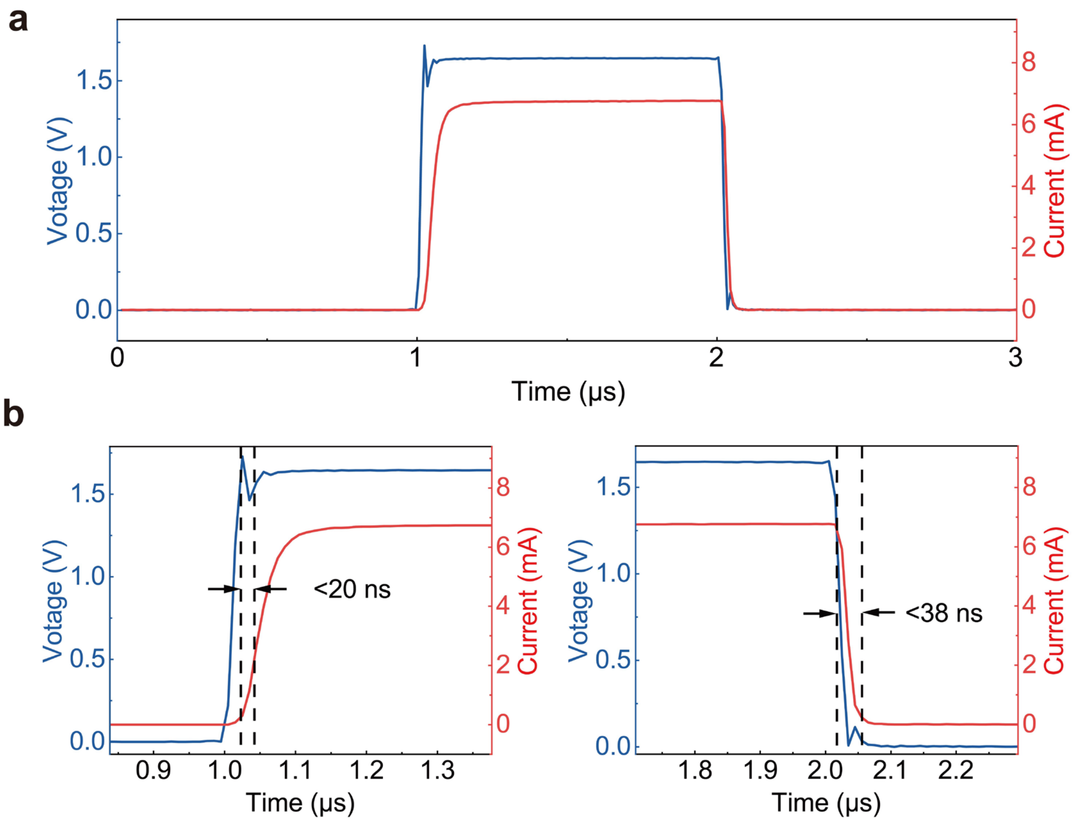

Supplementary Fig. 5. Transient switching response of the NbO_x memristor. a, The programmed voltage-pulse input (blue curve) and corresponding current response (red curve). **b,** The switching speed is < 20 ns from off-state to on-state (left) and is < 38 ns from on-state to off-state (right).

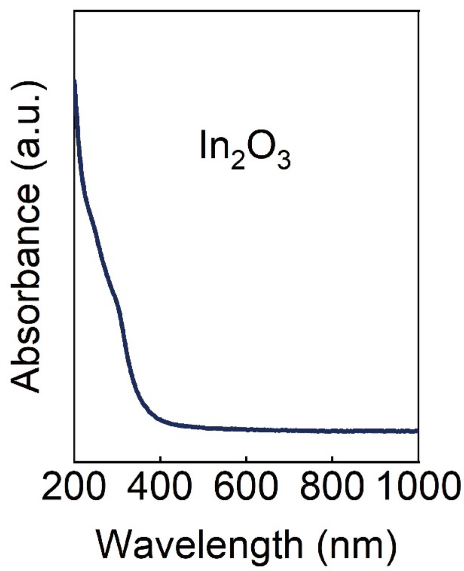

Supplementary Fig. 6. Ultraviolet-visible absorbance spectrum of In_2O_3 film.

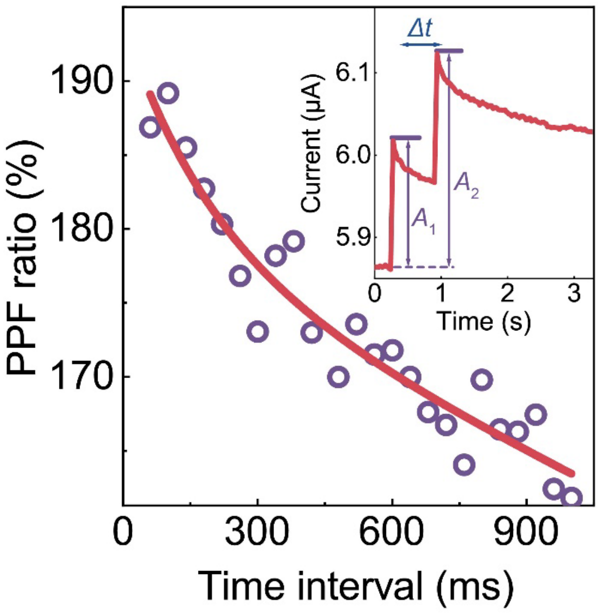

Supplementary Fig. 7. Paired pulse facilitation (PPF) ratio as a function of the optical pulse interval. The light intensity is 1.71 mW/cm^{-2} and the pulse width is 5 ms. PPF index is defined as $(A_2-A_1)/A_1\times100\%$, where the red line represents fitting results using the exponential decay function.

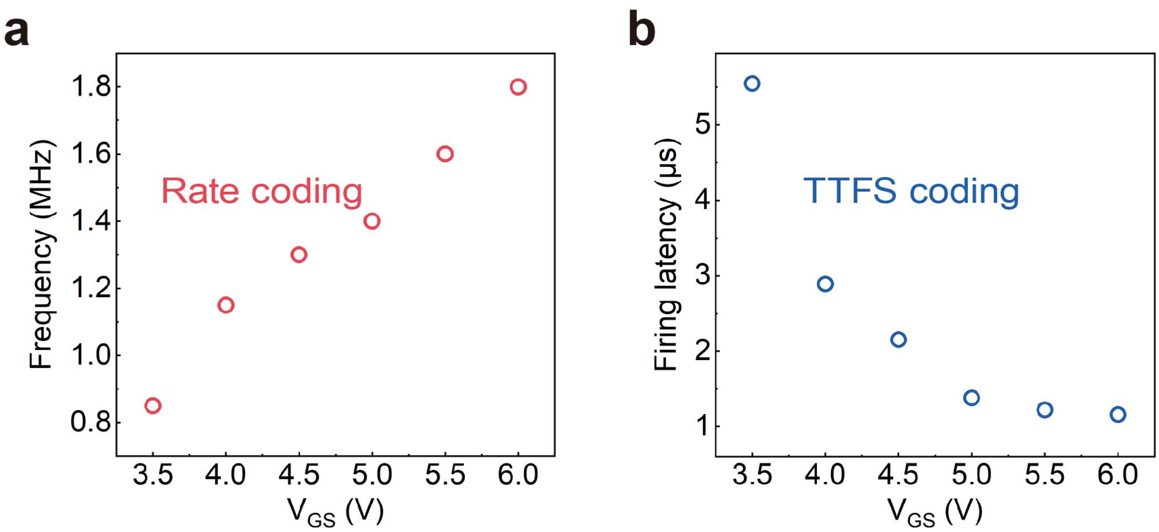

Supplementary Fig. 8. The effect of gate voltage on spike frequency and first spike latency.

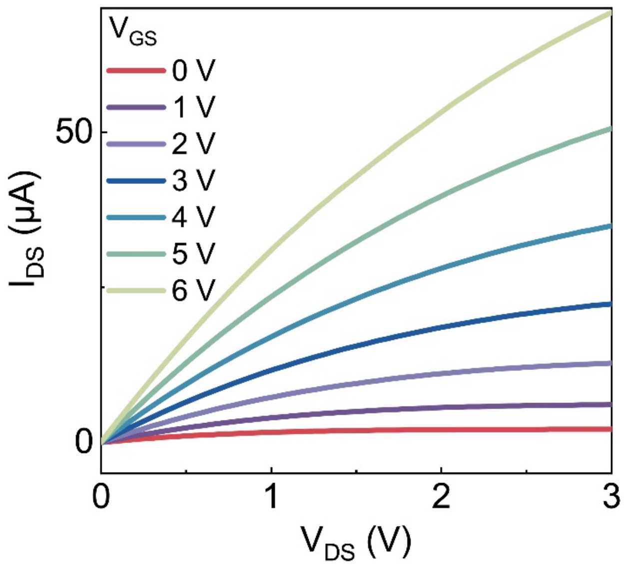

Supplementary Fig. 9. Output characteristics of optoelectronic synaptic transistor with V_G changed from 0 to 6 V in steps of 1 V.

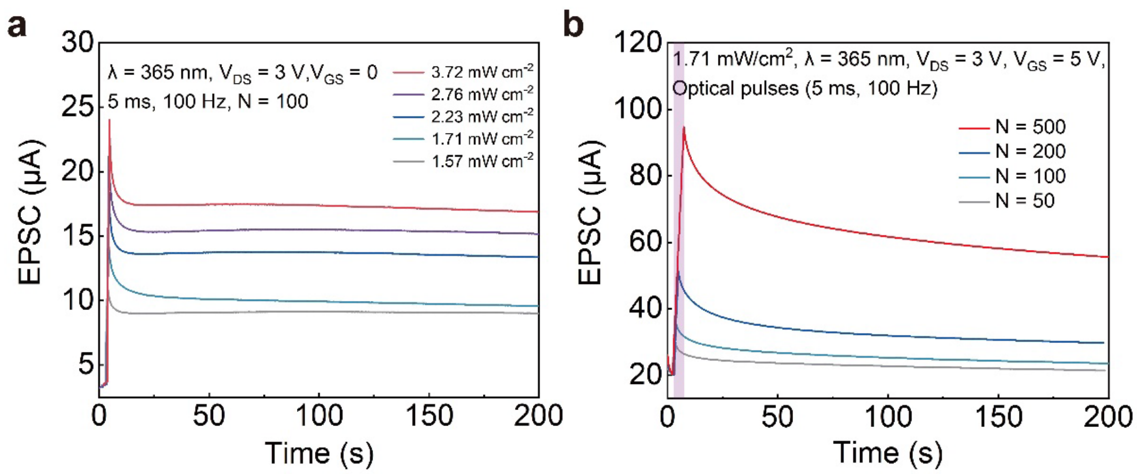

Supplementary Fig. 10. Synaptic plasticity under optical modulation. a, Excitatory postsynaptic current (EPSC) of the optoelectronic synaptic transistor triggered by various ultraviolet (UV) illumination intensities. **b,** EPSC of the optoelectronic synaptic transistor triggered by various UV light pulse numbers.

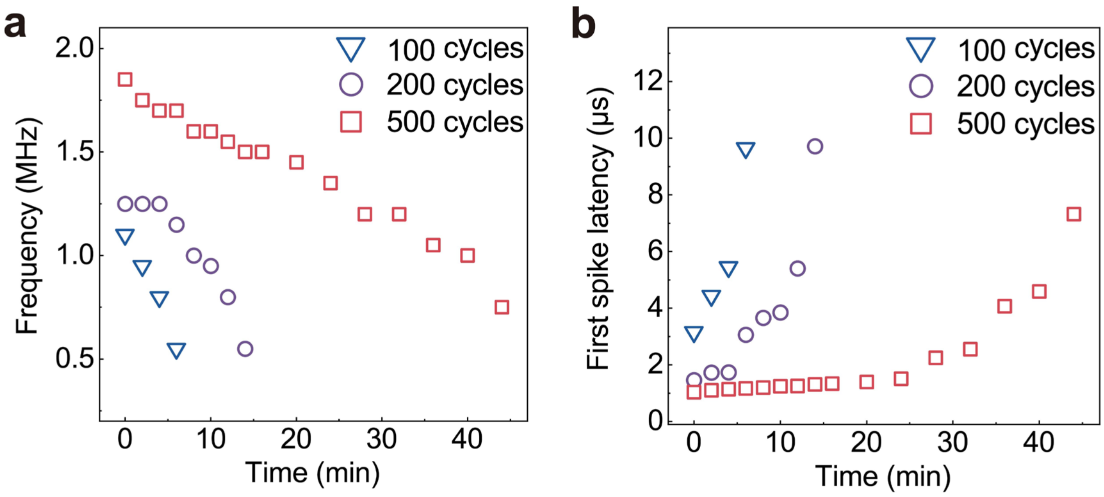

Supplementary Fig. 11. The rate-temporal fusion (RTF) coding performance over time in dark after UV light illumination with different pulse numbers. a, Change in spike frequency. **b,** Change in first spike latency.

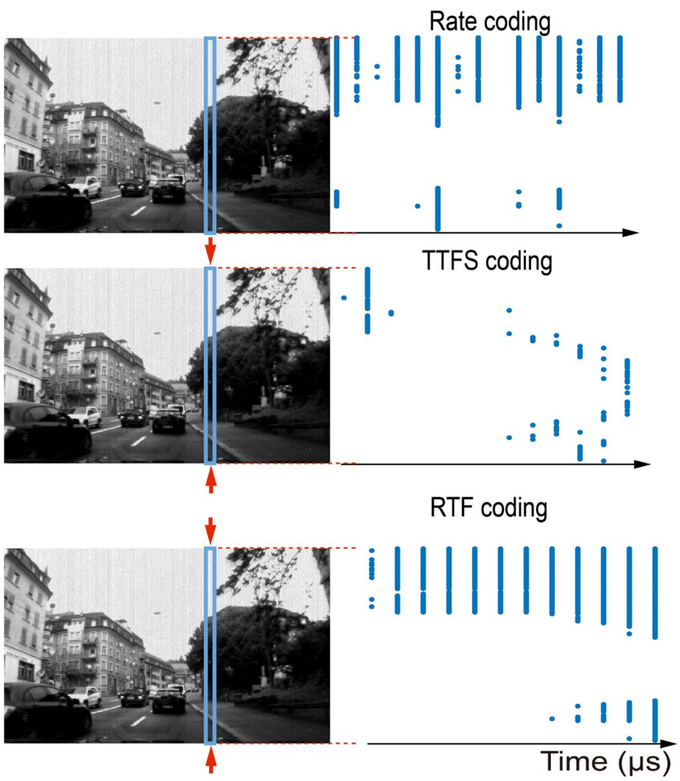

Supplementary Fig. 12. Spike raster of a self-driving recording image for rate coding, TTFS coding, and RTF coding in 15 time-steps. Spike trains of different coding methods for image locations along the column are marked by arrows.

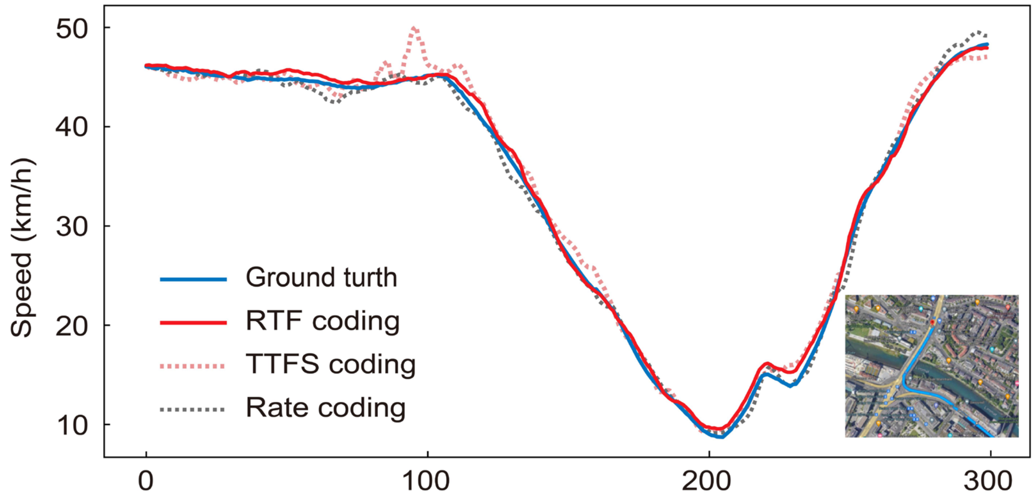

Supplementary Fig. 13. The comparison of speed prediction results of rate coding, TTFS coding, and RTF coding in complex road corners.

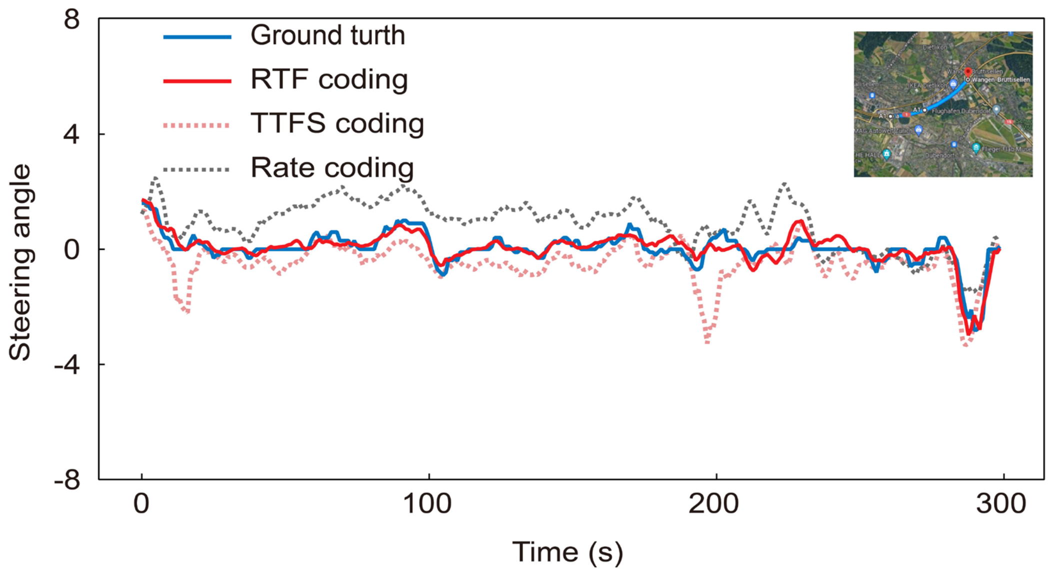

Supplementary Fig. 14. The comparison of steering angle prediction results of rate coding, TTFS coding and RTF coding in smooth road corner.

Supplementary Table 1. Comparison of different artificial spiking visual neurons.

Materials	Mechanism	Components	Switching/Relaxation speed	Endurance	Ref.
Two-dimensional b-AsP/$MoTe_2$	Optoelectronic	1T	NA	NA	1
Metal oxide	Filament-based	1D1T	40/55 ns	>500	2
Silicon	Electronic	CMOS circuit	NA	NA	3
Silicon	Optoelectronic	1T	NA	NA	4
Metal oxide	Filament-based	$2R1C1R_M$	10/40 ns	>1000	5
Metal oxide	Filament-based	$1R1C2R_M$	16/21 ns	>50	6
Monolayer MoS_2	Optoelectronic	21T	NA	NA	7
Metal oxide	**Mott transition**	**$1T1R_M$**	**20/38 ns**	**$>10^{10}$**	**This work**

Abbreviations: Transistor (T), diode (D), resistor (R), capacitor (C), memristor (R_M).

Supplementary Table 2. Comparison of characteristics of various artificial spiking visual neurons.

Neuron coding			Excitatory and inhibitory	Spike integration	Synaptic plasticity	Spiking frequency (Hz)	Spiking time resolution (s)	Energy/spike	Ref.
Rate	TTFS	TRF							
Yes	No	No	No	No	No	$0\text{-}10^5$	No	NA	1
Yes	No	No	No	Yes	No	0.1-1200	No	~40 pJ	2
No	Yes	No	Yes	Yes	Yes	9.6	~0.23	~93 mJ	3
Yes	No	No	Yes	Yes	No	35-60	No	~6.8 nJ	4
Yes	No	No	No	Yes	No	1-200	No	~2.5 nJ	5
Yes	No	No	No	Yes	Yes	0-160	No	NA	6
No	Yes	No	No	Yes	No	No	0.7	0.1-1 μJ	7
Yes	**Yes**	**Yes**	**Yes**	**Yes**	**Yes**	**$(0.35\text{-}1.85) \times 10^6$**	**1.04×10^{-6}**	**1.06 nJ**	**This work**

References

1 Wang, F. *et al.* A two-dimensional mid-infrared optoelectronic retina enabling simultaneous perception and encoding. *Nat. Commun.* **14**, 1938 (2023).

2 Wang, X. *et al.* Vertically integrated spiking cone photoreceptor arrays for color perception. *Nat. Commun.* **14**, 3444 (2023).

3 Kim, S. *et al*. Artificial stimulus-response system capable of conscious response. *Sci. Adv*. **7**, eabe3996 (2021).

4. Han J. K., et al. Bioinspired photoresponsive single transistor neuron for a neuromorphic visual system. *Nano. Lett.* **20**, 8781-8788 (2020).

5. Chen C., et al. A photoelectric spiking neuron for visual depth perception. *Adv. Mater.* **34**, e2201895 (2022).

6. Pei Y., et al. Artificial visual perception nervous system based on low-dimensional material photoelectric memristors. *ACS Nano* **15**, 17319-17326 (2021).

7. Subbulakshmi Radhakrishnan S., et al. A sparse and spike-timing-based adaptive photoencoder for augmenting machine vision for spiking neural networks. *Adv. Mater.* **34**, e2202535 (2022).